JACS
JOURNAL OF THE AMERICAN CHEMICAL SOCIETY

COMMUNICATION

pubs.acs.org/JACS

Spectroscopy of the Free Phenalenyl Radical

Gerard D. O'Connor,[†] Tyler P. Troy,[†] Derrick A. Roberts,[†] Nahid Chalyavi,[†] Burkhard Fückel,[†] Maxwell J. Crossley,[†] Klaas Nauta,[†] John F. Stanton,[‡] and Timothy W. Schmidt*[,†]

[†]School of Chemistry, The University of Sydney, New South Wales 2006, Australia

[‡]Department of Chemistry and Biochemistry, The University of Texas at Austin, 1 University Station A5300, Austin, Texas 78712-0165, United States

Supporting Information

ABSTRACT: After benzene and naphthalene, the smallest polycyclic aromatic hydrocarbon bearing six-membered rings is the threefold-symmetric phenalenyl radical. Despite the fact that it is so fundamental, its electronic spectroscopy has not been rigorously scrutinized, in spite of growing interest in graphene fragments for molecular electronic applications. Here we used complementary laser spectroscopic techniques to probe the jet-cooled phenalenyl radical in vacuo. Its spectrum reveals the interplay between four electronic states that exhibit Jahn−Teller and pseudo-Jahn−Teller vibronic coupling. The coupling mechanism has been elucidated by the application of various ab initio quantum-chemical techniques.

The phenalenyl radical consists of three six-membered rings that share a central carbon atom (Figure 1 inset). As a 13-carbon conjugated species, the neutral form is a resonance-stabilized radical. Resonance-stabilized radicals are found to form spontaneously in electrical discharges and recognized as important intermediates in fuel-rich combustion.[1,2] Indeed, the phenalenyl radical is so stabilized by resonance that it can be generated and observed at room temperature in solution.[3] The phenalenyl radical motif has been extensively invoked in the design of organic molecular conductors[4] and is a prototypical open-shell graphene fragment.[5]

Astronomically it is posited to be partly responsible for the extended red emission, a red glow associated with carbon-rich nebulae.[6] The recent discovery of fullerenes in a young planetary nebula[7] has reinvigorated the search for other polycyclic conjugated species in space. Indeed, polycyclic aromatic hydrocarbons have long been held to be responsible for strong IR emission bands observed in a range of interstellar environments.[8]

Despite much attention, a detailed understanding of the electronic structure and spectroscopy of this fundamental species is still lacking. Highly resolved fluorescence excitation and emission spectra of the radical in a cryogenic matrix were reported previously but with no satisfactory analysis.[9] The spectrum of the gas-phase phenalenyl radical has not been reported to date. To compare with absorption spectra of the interstellar medium or probe for its production in complex chemical environments, such a measurement is required. We have obtained the first electronic spectra of the phenalenyl radical under rigorously isolated conditions through laser interrogation of a molecular beam. Analysis of the spectrum revealed the influence of Jahn−Teller (JT) and pseudo-JT effects[10] and manifestations of the Coulson−Rushbrooke pairing theorem.[11]

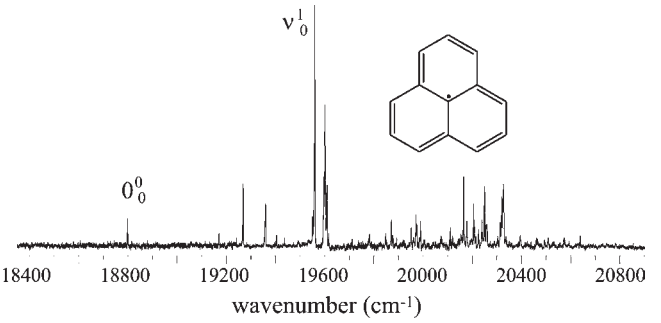

Figure 1. Resonant ionization spectrum of phenalenyl radical (m/z 165). The inset shows a resonance structure of phenalenyl radical.

The excitation spectrum of phenalenyl radical obtained by resonant two-color two-photon ionization is shown in Figure 1. The origin (0_0^0) is observed to be much weaker than the vibronic features near 19600 cm^{-1} (labeled ν_0^1). Our excitation spectrum is nearly identical to that observed by Cofino et al.[9] in cryogenic matrices but is blue-shifted by ∼130 cm^{-1}. Comparison to condensed-phase emission confirmed the assignment of the origin.

The molecule thus exhibits a propensity for changing one quantum in ν (780 cm^{-1}) upon making an electronic transition (note that this is not necessarily meant in the usual Franck−Condon sense). This is further exhibited by single-vibronic-level fluorescence emission spectra obtained by exciting the origin and the ν_0^1 band (Figure 2). Emission from the vibrationless level is predominantly to one quantum in a mode with a frequency similar to ν, and emission from the state prepared by pumping ν_0^1 is predominantly to twice this frequency (i.e., two quanta of ν). Such behavior is reminiscent of vibrational spectroscopy, where the selection rule is $\Delta n = \pm 1$. This behavior is manifested in vibronic spectra as the Herzberg−Teller effect. To elucidate the mechanism of the observed spectra, one must consider the electronic structure.

The electronic structure of the phenalenyl radical has attracted much interest from the standpoint of molecular electronics and studies of aromaticity. The perimeter of the radical is antiaromatic, having 12 π electrons distributed among 12 p orbitals. The perimeter orbitals can be represented as cosine and sine waves multiplied by the unhybridized p orbitals. The degenerate highest-occupied perimeter orbitals have a periodicity of 3, as shown in Scheme 1. One of these exhibits nodes on the bonds joining the periphery to the central carbon, and the

Received: July 8, 2011
Published: August 20, 2011

dx.doi.org/10.1021/ja206322n | J. Am. Chem. Soc. 2011, 133, 14554–14557

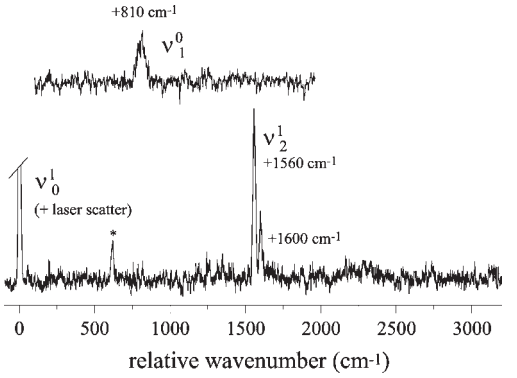

Figure 2. Single-vibronic-level emission spectra of the phenalenyl radical resulting from excitation of the (top) 0_0^0 and (bottom) ν_0^1 bands in Figure 1. In the latter, the small feature at +1600 cm^{-1} is likely due to Fermi resonance; the feature marked with an asterisk is unassigned.

Scheme 1. Schematic Explaining the Stabilization of the 13-π-Electron System[a]

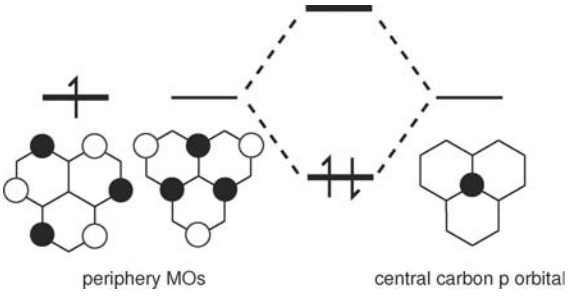

[a] The antiaromatic periphery orbitals (left) differ in phase, and only one can interact with the central p orbital (right). This interaction produces new MOs, one of which stabilizes the structure. Thus, the radical electron remains on the periphery, and the 12-π-electron cation is aromatic.

other possesses antinodes in these positions. This latter orbital interacts with the central p orbital to give new molecular orbitals (MOs), one being stabilized. Thus, the radical electron is left in a peripheral orbital (despite the resonance structure shown in the Figure 1 inset). Indeed, according to Hückel theory, the stabilized orbital becomes degenerate with the next-lowest π MOs. As such, although the cation has 12 electrons, it is a stable aromatic system and has been described as a "magnetic chameleon".[12]

The predictions of Hückel theory are largely borne out by higher-level calculations, with the ground-state neutral predicted to have $^2A_1''$ symmetry. Being nondegenerate, the D_{3h} geometry should be stable, as supported by a density functional theory (DFT) calculation of the ground state. At the restricted open-shell Hartee–Fock (ROHF) level, the orbitals immediately higher and lower than the a_1'' singly occupied MO (SOMO) have e″ symmetry, with the a_2'' orbitals resulting from the interaction shown in Scheme 1 being the next highest and lowest (Figure 3). The first excited electronic states are therefore expected to have E″ symmetry. The pure electronic transition $E'' \leftarrow A_1''$ is allowed, being polarized in the plane of the molecule ($\Gamma_\mu = e'$). The origin is thus expected to be observable, as seen above. Now, transitions to single quanta of both a_1' and e′ modes in the E″ excited electronic state are both allowed ($E'' \otimes e' \supset E''$), so we may attempt to assign the modes labeled ν in Figures 1 and 2 by these considerations. At the DFT geometry, a complete-active-space calculation using the ROHF orbitals was performed.

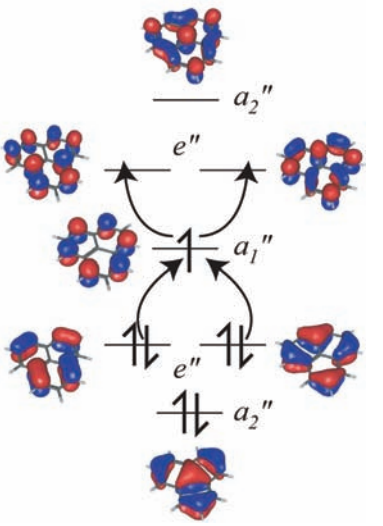

Figure 3. ROHF frontier orbitals of the phenalenyl radical. The lower a_2'' orbital is derived from one of the peripheral orbitals in Scheme 1. The four single-electron transitions that give rise to the two pairs of E″ states are indicated.

In this space, the first excited electronic states are indeed found to have E″ symmetry, and these are herein denoted $1^2E''$. Corrections for more highly excited determinants using multireference second-order perturbation theory place the $1^2E''$ state at 2.1 eV, compared to the observed value of 2.3 eV.

The emission from the vibrationless level of the $1^2E''$ state peaks at 810 cm^{-1}. This appears to correspond to a mode of e′ symmetry, ν_{25}, which is calculated by DFT to have a frequency of 811 cm^{-1} after scaling by 0.97, a factor that we have determined from a number of previous studies of resonance-stabilized hydrocarbon radicals to yield excellent agreement with experimental ground-state frequencies.[1] The nearest competing assignment is an a_1' mode predicted to have a frequency of 766 cm^{-1}.

According to the JT theorem,[10] distortion along the e′ mode ν_{25} lifts the degeneracy of the $1^2E''$ state, giving C_{2v} symmetry along one component of ν_{25} and C_s symmetry along the other. In the C_{2v} point group, these components have a_1 and b_2 symmetry, respectively, and we label them here Q_a and Q_b. By distorting the geometry along Q_a, we can investigate the JT effect by calculating the splitting of the $1^2E''$ state into A_2 and B_1 components in the reduced C_{2v} symmetry. The surfaces thus generated are displayed in Figure 4. The splitting is relatively small, with the zero-point energy of the two-dimensional oscillator lying well above the point of degeneracy.

The JT effect can introduce intensity in the vibronic transitions to states that correspond to a single quantum of excitation in the e′ modes in this molecule. To test whether the JT coupling is responsible for the vastly increased intensity of 25_0^1 relative to the origin, we solved the vibronic problem in the diabatic electronic basis, where the electronic states retain C_{2v} symmetry and the kinetic energy matrix is diagonal. The linear JT electronic Hamiltonian is

$$\mathbf{V} = \begin{bmatrix} \lambda_1\rho^2 & 0 & 0 \\ 0 & \Delta_2 + \lambda_2\rho^2 - kQ_a & +kQ_b \\ 0 & +kQ_b & \Delta_3 + \lambda_3\rho^2 + kQ_a \end{bmatrix}$$

where the the harmonic potentials λ_i are taken to be equivalent, k is taken from the calculated slope of the conical intersection displayed in Figure 4, and $\rho^2 = Q_a^2 + Q_b^2$. The terms $\Delta_2 = \Delta_3$

dx.doi.org/10.1021/ja206322n |J. Am. Chem. Soc. 2011, 133, 14554–14557

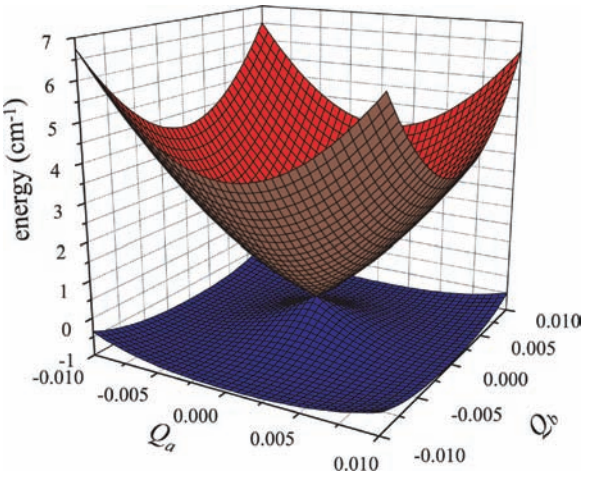

Figure 4. Adiabatic potential energy curves associated with the $1^2E''$ electronic state as a function of the components of the e′ mode ν_{25}.

represent the electronic energy of the $1^2E''$ state at the ground-state equilibrium geometry. Diagonalization of **V** regenerates the adiabatic potentials in Figure 4. With a ground state 2D harmonic oscillator basis, the calculated energy levels reveal a JT splitting of only 4 cm^{-1} in the $\nu_{25} = 1$ levels and much less intensity in the 25_0^1 peak than in the origin. As such, the JT effect in the $1^2E''$ manifold cannot be held responsible for the observed intensity pattern.

As mentioned above, intensity in modes that are not totally symmetric is often associated with the Herzberg−Teller effect, whereby the slope of the transition dipole moment induces a coupling between vibronic states differing by one quantum in the mode of interest. The smooth evolution of the electronic transition moment with geometry is a manifestation of the adiabatic Born−Oppenheimer approximation, which is known to be invalid for JT-coupled electronic states. Nevertheless, we may calculate the transition moment to the components of the $1^2E''$ state for distortions along Q_a. As an a_1 mode in C_{2v}, this preserves the A_2 and B_1 symmetries of the adiabatic states. The results of this calculation are displayed in Figure 5, which shows a substantial slope of the transition moments with respect to distortion along Q_a, indicating a strong mixing with another state along the adiabat. For excited states without conical intersections, the transition moment can be calculated adiabatically, and the resulting function of the geometry can be used to model the excitation spectrum in terms of the Herzberg−Teller effect.[13] However, we cannot calculate the transition moments adiabatically, as they are not single-valued. To understand why, we can consider an adiabatic "walk" around the minimum in the potential in Figure 4. By traversing π radians from $Q_a > 0$, $Q_b = 0$ and arriving at $Q_b = 0$, one crosses from one of the C_{2v} diabatic states to the other. The adiabats may be expressed as

$$|2^{ad}\rangle = \cos(\theta/2)|2^{d}\rangle + \sin(\theta/2)|3^{d}\rangle$$

$$|3^{ad}\rangle = -\sin(\theta/2)|2^{d}\rangle + \cos(\theta/2)|3^{d}\rangle$$

where the superscripts "ad" and "d" indicate adiabatic and diabatic states, respectively. From these expressions, it is clear that a full traversal of 2π radians would result in a change of sign of the wave function and thus of the transition moment. This problem, known as the Berry phase[14] (or geometric phase), may

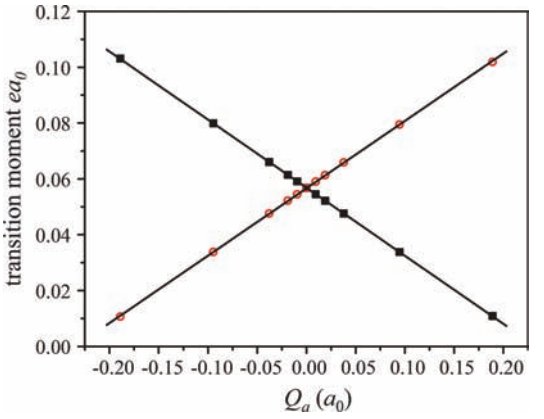

Figure 5. Adiabatic transition moments to the $1^2E''$ manifold as functions of distortion along Q_a.

be eliminated by using a diabatic basis. Accordingly, we must identify the origin of the transition moment derivative.

The frontier MOs are illustrated in Figure 3. The manifestation of the Coulson−Rushbrooke pairing theorem is apparent, the orbitals being paired between π and π^* orbitals differing by a sign change on alternant carbon atoms.[11] There are four single-electron transitions that give rise to four excited configurations. These pairs of configurations are calculated to interact to give rise to two pairs of E″ states as even and odd combinations of the excited configurations. In cases such as these, with odd-alternant π systems, not only are the energies of the excited configurations identical at the Hückel level, but so are their transition moments.[14,15] As a consequence, there is a near cancelation of the transition moment for the $1^2E'' \leftarrow {}^2A_1''$ transition and constructive interference for the $2^2E'' \leftarrow {}^2A_1''$ transition.[16] Indeed, the latter transition moments are $\sim 2.5ea_0$ at the equilibrium position. The steep change in transition moment seen in Figure 5 is due to vibronic coupling to the upper, bright $2^2E''$ states.

To model the interaction of these four E″ states in the diabatic representation, we invoked pseudo-JT off-diagonal terms. The electronic Hamiltonian is now

$$\mathbf{V} = \begin{bmatrix} V_{11} & 0 & 0 & 0 & 0 \\ 0 & V_{22} - kQ_a & +kQ_b & +gQ_a & +gQ_b \\ 0 & +kQ_b & V_{33} + kQ_a & +gQ_b & -gQ_a \\ 0 & +gQ_a & +gQ_b & V_{44} - fQ_a & +fQ_b \\ 0 & +gQ_b & -gQ_a & +fQ_b & V_{55} + fQ_a \end{bmatrix}$$

where the parameters k, f, and g are calculated from analytical diabatic couplings using the EOM−CCSD method.[17] The diagonal potentials are given by $V_{ii} = \Delta_i + \lambda_i\rho^2$. Solving the vibronic problem in a harmonic oscillator basis yields eigenvectors $|\Psi\rangle$. The excitation spectrum is obtained by plotting the square of the vibronic transition moment, $|\langle\Psi'|M|\Psi''\rangle|^2$, where M is the electronic transition dipole moment matrix in the diabatic representation evaluated at the D_{3h} geometry projected onto the C_{2v} components. The calculated spectrum is shown in Figure 6, and the resemblance to the experimental spectrum in Figure 1 is clear. This demonstrates that the effect of the pseudo-JT coupling between the $1^2E''$ and $2^2E''$ manifolds is responsible for the observed intensity pattern. A more detailed treatment is planned for a future publication.

Spectra of PAH radicals of this size are of interest for comparison to diffuse interstellar bands (DIBs).[18] In

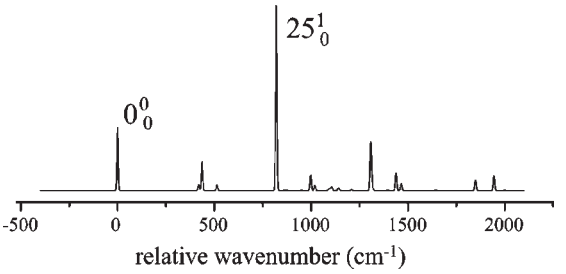

Figure 6. Spectrum calculated using the vibronic Hamiltonian including JT and pseudo-JT coupling, with EOM−CCSD-computed coupling constants. An intensity pattern closely resembling Figure 1 is observed.

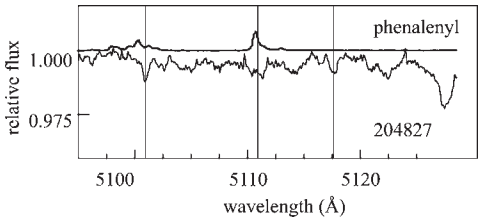

Figure 7. Comparison of the phenalenyl radical excitation spectrum and the spectrum toward HD204827.[21] Vertical lines indicate DIBs.

particular, the phenalenyl radical is a worthy candidate because of its aromatic stabilization. Benzene is a known circumstellar molecule,[19] and there is evidence for the naphthalene cation in space.[20] The next largest PAH with six-membered rings is phenalenyl radical. A comparison of the observed excitation spectrum to the DIBs observed in the star HD204827[21] is shown in Figure 7. The strongest band of the phenalenyl radical coincides with a rather weak DIB, with the other strong band plausibly lost in the complicated astronomical spectrum. While this is tenuous evidence at best for interstellar phenalenyl radical, the existence of much stronger $2^2E'' \leftarrow {}^2A_1''$ transitions compels us to return to the laboratory to search for the associated band system, which would be much more likely to be observable in the spectra of the interstellar medium.

In conclusion, we have obtained the first spectra of the phenalenyl radical under rigorously isolated conditions in a molecular beam. Theoretical considerations indicate that the transition observed here is $1^2E'' \leftarrow A_1''$ in symmetry, with the upper state strongly coupled (via the pseudo-JT mechanism) to the $2^2E''$ state. The latter carries nearly all of the oscillator strength arising from transitions between the frontier orbitals. There is a coincidence between the strongest band and a weak interstellar absorption feature, but the prediction of much stronger $2^2E'' \leftarrow A_1''$ transitions compels us to search for these in the laboratory.

■ ASSOCIATED CONTENT

Supporting Information. Experimental and computational details. This material is available free of charge via the Internet at http://pubs.acs.org.

■ AUTHOR INFORMATION

Corresponding Author
timothy.schmidt@sydney.edu.au

■ ACKNOWLEDGMENT

This research was supported under the Australian Research Council (ARC) (Project DP0985767). T.P.T. acknowledges The University of Sydney for a University Postgraduate Award. N.C. acknowledges the Endeavor International Postgraduate Research Scholarship and the University of Sydney International Scholarship. B.F. acknowledges a Feodor Lynen Fellowship from the Alexander von Humboldt Foundation. K.N. thanks the ARC for an Australian Research Fellowship. J.F.S. thanks the U.S. National Science Foundation and the Robert A. Welch Foundation (Grant F-1283) for support. The authors thank Scott Reid and Scott Kable for critical reading of the manuscript and Audrey Stanton for composing the TOC graphic.

■ REFERENCES

(1) (a) Reilly, N. J.; Kokkin, D. L.; Nakajima, M.; Nauta, K.; Kable, S. H.; Schmidt, T. W. *J. Am. Chem. Soc.* **2008**, *130*, 3137. (b) Reilly, N. J.; Nakajima, M.; Troy, T. P.; Chalyavi, N.; Duncan, K. A.; Nauta, K.; Kable, S. H.; Schmidt, T. W. *J. Am. Chem. Soc.* **2009**, *131*, 13423.

(2) da Silva, G.; Bozzelli, J. W. *J. Phys. Chem. A* **2009**, *113*, 12045.

(3) Goto, K.; Kubo, T.; Yamamoto, K.; Nakasuji, K.; Sato, K.; Shiomi, D.; Takui, T.; Kubota, M.; Kobayashi, T.; Yakusi, K.; Ouyang, J. Y. *J. Am. Chem. Soc.* **1999**, *121*, 1619.

(4) (a) Pal, S. K.; Bag, P.; Sarkar, A.; Chi, X.; Itkis, M. E.; Tham, F. S.; Donnadieu, B.; Haddon, R. C. *J. Am. Chem. Soc.* **2010**, *132*, 17258. (b) Pal, S. K.; Itkis, M. E.; Tham, F. S.; Reed, R. W.; Oakley, R. T.; Haddon, R. C. *Science* **2005**, *309*, 281. (c) Itkis, M. E.; Chi, X.; Cordes, A. W.; Haddon, R. C. *Science* **2002**, *296*, 1443. (d) Haddon, R. C. *Nature* **1975**, *256*, 394. (e) Haddon, R. C. *Aust. J. Chem.* **1975**, *28*, 2343. (f) Dutta, P.; Maiti, S. K.; Karmakar, S. *Org. Electron.* **2010**, *11*, 1120.

(5) Morita, Y.; Suzuki, S.; Sato, K.; Takui, T. *Nat. Chem.* **2011**, *3*, 197.

(6) Rhee, Y. M.; Lee, T. J.; Gudipati, M. S.; Allamandola, L. J.; Head-Gordon, M. *Proc. Natl. Acad. Sci. U.S.A.* **2007**, *104*, 5274.

(7) Cami, J.; Bernard-Salas, J.; Peeters, E.; Malek, S. E. *Science* **2010**, *329*, 1180.

(8) Leger, A.; Puget, J. L. *Astron. Astrophys.* **1984**, *137*, L5.

(9) Cofino, W. P.; van Dam, S. M.; Kamminga, D. A.; Hoornweg, G.; Gooijer, C.; MacLean, C.; Velthorst, N. H. *Mol. Phys.* **1984**, *51*, 537.

(10) Jahn, H. A.; Teller, E. *Proc. R. Soc. London, Ser. A* **1937**, *161*, A905.

(11) Coulson, C.; Rushbrooke, G. *Proc. Cambridge Philos. Soc.* **1940**, *36*, 193.

(12) Cyrański, M. K.; Havenith, R. W. A.; Dobrowolski, M. A.; Gray, B. R.; Krygowski, T. M.; Fowler, P. W.; Jenneskens, L. W. *Chem.—Eur. J.* **2007**, *13*, 2201.

(13) Chang, C.-H.; Lopez, G.; Sears, T. J.; Johnson, P. M. *J. Phys. Chem. A* **2010**, *114*, 8262.

(14) Berry, M. V. *Proc. R. Soc. London, Ser. A* **1984**, *392*, 45.

(15) Ding, H.; Schmidt, T. W.; Pino, T.; Boguslavskiy, A. E.; Güthe, F.; Maier, J. P. *J. Chem. Phys.* **2003**, *119*, 814.

(16) Longuet-Higgins, H. C.; Pople, J. A. *Proc. R. Soc. London, Ser. A* **1955**, *68*, 591.

(17) Ichino, T.; Gauss, J.; Stanton, J. *J. Chem. Phys.* **2009**, *130*, No. 174105.

(18) Sarre, P. J. *J. Mol. Spectrosc.* **2006**, *238*, 1.

(19) Cernicharo, J.; Heras, A. M.; Tielens, A. G. G. M.; Herpin, J. R. P. F.; Guélin, M.; Waters, L. B. F. M. *Astrophys. J.* **2001**, *546*, L123.

(20) Iglesias-Groth, S.; Manchado, A.; García-Hernández, D. A.; Hernández, J. I. G.; Lambert, D. L. *Astrophys. J.* **2008**, *685*, L55.

(21) Hobbs, M.; York, D. G.; Snow, T. P.; Oka, T.; Thorburn, J. A.; Bishof, M.; Friedman, S. D.; McCall, B. J.; Rachford, B.; Sonnentrucker, P.; Welty, D. E. *Astrophys. J.* **2008**, *680*, 1256.